Electronic phase transition of the valence-fluctuating fulleride $Eu_{2.75}C_{60}$

Yusuke Yamanari,[1] Yuta Suzuki,[1] Kumiko Imai,[2] Eiji Shikoh,[3,*] Akihiko Fujiwara,[3,†] Naoko Kawasaki,[2] Naoshi Ikeda,[1] Yoshihiro Kubozono,[2] and Takashi Kambe[1,‡]

[1]*Department of Physics, Okayama University, Okayama 700-8530, Japan*

[2]*Reserach Laboratory for Surface Science, Okayama University, Okayama 700-8530, Japan*

[3]*Japan Advanced Institute of Science and Technology, Ishikawa, 923-1292, Japan*

(Received 17 February 2010; revised manuscript received 28 March 2011; published 3 June 2011)

The electronic properties of $Eu_{2.75}C_{60}$ are studied using magnetic susceptibility and electron spin resonance (ESR) from 2 to 300 K. Both the magnetic susceptibility and the ESR parameters clearly show an anomaly around the valence transition temperature, $T_V = 70$ K. The magnetic susceptibility shows weak temperature dependence above T_V, while it changes drastically to Curie-Weiss behavior below T_V. The low-temperature susceptibility can be reproduced by assuming the moment of free Eu^{2+} ions. This result reveals that $Eu_{2.75}C_{60}$ changes from the intermediate valence state to the divalent state below T_V. Although ESR signals above T_V should be attributed to conduction electrons, the ESR intensity below T_V follows the Curie-Weiss law with a distinct increase in the g-factor. This should be associated with a strong localization of π electrons. We also found that, below $\sim$17 K, the isothermal magnetization exhibits a weak hysteresis and thermoremanent magnetization appears. These results suggest that valence-ordered $Eu_{2.75}C_{60}$ undergoes antiferromagnetic ordering with a weak ferromagnetic component at the Néel temperature, $T_N = 17$ K.

DOI: 10.1103/PhysRevB.83.245103 PACS number(s): 71.20.Tx, 71.30.+h, 75.30.Kz, 75.30.Mb

I. INTRODUCTION

The superconducting properties of metal-doped C_{60} materials, in which metal atoms are intercalated into the C_{60} crystal lattice, have been extensively studied by many investigators.[1–6] The highest reported superconducting transition temperature T_c is now 33 K for $RbCs_2C_{60}$ under ambient pressure,[2] while the highest T_c under high pressure is 40 K for Cs_3C_{60}.[6] This pressure-induced superconductivity of Cs_3C_{60} was controversial during the past decade,[7–9] but very recently Ganin *et al*. determined that the A15 phase of Cs_3C_{60} is the superconducting phase under pressure.[10,11] Furthermore, metal-doped C_{60} materials exhibit very interesting electronic phases, including a metallic phase and a ferromagnetic phase.[3] The low-dimensional polymer phases in alkali-metal-doped C_{60} show a variety of metal-insulator transitions.[12–14] Thus, metal-doped C_{60} materials present an interesting entry point for the exploration of solid state physics.

C_{60} materials with intercalated lanthanide-metal atoms and the endohedral structures in which Ln is encapsulated inside the C_{60} cage (Ln@C_{60}, where Ln is the lanthanide atom) were first investigated during the past decade,[15–17] and their electronic structures were partly clarified.[18,19] Furthermore, an opening of an energy gap at 28 K is suggested by scanning tunneling microscopy of a single C_{60}-encapsulated La cluster (i.e., La@C_{60}),[19] which is suggested to be metallic. Subsequently, lanthanide-metal-doped C_{60} materials were studied and superconducting properties were reported for Sm_xC_{60} ($T_c = 8$ K).[20] Furthermore, a unique physical property (i.e., a valence fluctuation of the doped metal atom) was clarified for $Sm_{2.75}C_{60}$.[21–23] A temperature-induced valence transition in Sm was first found in $Sm_{2.75}C_{60}$, and a negative thermal expansion was observed below the valence transition temperature. At high temperatures, the valence of the Sm atom fluctuates between +2 and +3, while the fraction of Sm^{2+} increases with decreasing temperature. The larger ionic radius of Sm^{2+} (0.114 nm) than Sm^{3+} (0.096 nm) induces the negative thermal expansion at low temperature. Prassides *et al*. clearly showed that the electronic state of $Sm_{2.75}C_{60}$ at room temperature was the mixed valence state of Sm^{2+} and Sm^{3+} and that the fraction of Sm^{2+} was 70%.[21] They clarified that the fraction of Sm^{2+} gradually increased down to 40 K, then rapidly increased as the temperature decreased below 40 K. The increase in the fraction of Sm^{2+} produces the negative thermal expansion. Furthermore, at room temperature, a pressure-induced rapid decrease in volume was observed above 4 GPa, which was attributed to the valence variation of Sm from +2.3 to +3.[22] $Eu_{2.75}C_{60}$ and $Yb_{2.75}C_{60}$ also show the same valence transition as $Sm_{2.75}C_{60}$ (i.e., a similar negative thermal expansions were reported[23]). The transition temperature for this thermal-expansion anomaly was 90 K for $Eu_{2.75}C_{60}$ and 60 K for $Yb_{2.75}C_{60}$. Thus, both valence variation and negative thermal expansion are characteristic of lanthanide-metal-doped C_{60} materials.

Here we have studied the electronic and magnetic properties of $Eu_{2.75}C_{60}$ using its magnetic susceptibility and temperature-dependent electron spin resonance (ESR) spectra. A drastic change in magnetic susceptibility and ESR parameters was observed at the electronic transition temperature, and the change in magnetic susceptibility and ESR will be discussed on the basis of the valence transition of Eu in $Eu_{2.75}C_{60}$.

II. EXPERIMENTAL DETAILS

Eu_xC_{60} samples were synthesized by the thermal reaction of Eu and C_{60} in Ta tubes. Nominal amounts of Eu and C_{60} were introduced into Ta tubes in an Ar glove box ($O_2 <$ 0.1 ppm and $H_2O <$ 0.1 ppm), and these tubes were inserted into quartz tubes. The quartz tubes were sealed after dynamic pumping to 10^{-6} Torr. The tubes were then heated at 420 °C for about 1 month. The target samples obtained were introduced into glass capillaries for x-ray diffraction measurements and into quartz tubes for ESR and magnetic measurements. The exact chemical compositions of Eu_xC_{60} were determined from

powder x-ray diffraction patterns measured with synchrotron radiation at beam line BL-1B of the Photon Factory of the High Energy Acceleration Research Organization (KEK-PF), Tsukuba, Japan with $\lambda = 0.99\,937$ Å. Temperature-dependent ESR spectra were measured with an *X*-band ESR spectrometer (Bruker ESP-300) equipped with a He-flow cryostat (Oxford Instrument ESR910). The ESR spectral parameters were determined by least-squares fitting with multiple components of Lorentz functions. The ESR signals at all temperatures were completely investigated by the Lorentz functions. To investigate the absolute value of the spin susceptibility, we examined the ESR experiments at the *X*-band and *Q*-band. No considerable difference in susceptibility between the two frequencies is found. The static susceptibility was measured with a superconducting quantum interference device (SQUID) magnetometer (Quantum Design MPMS2).

III. RESULTS AND DISCUSSIONS

Figure 1(a) shows the diffraction patterns at 220 K. Black crosses and the red line show the observed and calculated diffraction patterns, respectively, and the blue line shows the difference between the observed and calculated patterns. Pink vertical bars correspond to the predicted peak positions. The nominal concentration x was refined by the Le Bail refinements with the GSAS program[25] and was determined to be $x = 2.76$ at 295 K. The space group was *P*cab, and the lattice constants, a, b, and c at 220 K were 28.162(1), 28.125(1), and 28.142(1) Å,

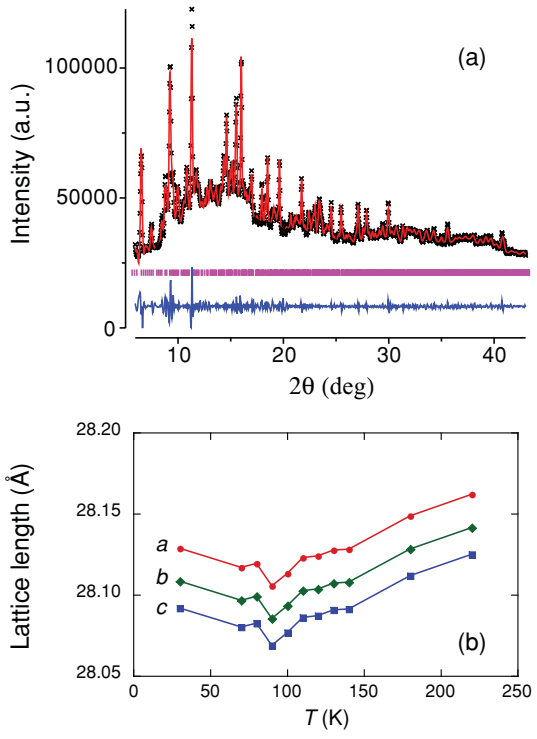

FIG. 1. (Color online) (a) X-ray diffraction spectrum of $Eu_{2.75}C_{60}$. The x-ray wavelength was 0.99 937 Å. Black crosses and the red line show the observed and calculated diffraction patterns, respectively, and the blue line shows the difference between the observed and calculated patterns. Pink vertical bars correspond to the predicted peak positions. (b) Temperature dependence of lattice constants.

respectively. These values are similar to those reported previously for $Sm_{2.75}C_{60}$ and $Yb_{2.75}C_{60}$.[21–24] Figure 1(b) shows the temperature dependence of the lattice parameters. From 295 to 90 K, all the crystal axes shrink monotonically with decreasing temperature. The thermal expansion rates, $\alpha_a[= \frac{1}{a}\frac{da}{dT}]$, α_b, and α_c along the a, b, and c axes are 1.39×10^{-5} K^{-1}, 1.38×10^{-5} K^{-1}, and 1.38×10^{-5} K^{-1}, respectively. These values are almost consistent with those of $Sm_{2.75}C_{60}$. However, below 90 K, all the crystal axes gradually expand with decreasing temperature. Thus, the negative thermal expansions are clearly observed. The transition seems to be first order because of the observation of thermal hysteresis (not shown).

Next, we discuss the mixed valence state at room temperature. Since a broad ESR signal, which may originate in the π conduction electrons (as shown later), is observed at 295 K, we have to take the contribution of Pauli paramagnetic susceptibility into account in order to estimate the Eu valence state. Thus, we try to estimate the Pauli paramagnetic contribution from the integrated ESR intensity, and then subtract it from the magnetic susceptibility obtained by SQUID measurements. The ground state of the Eu^{3+} multiplet is $^7F_0$ ($4f^6$; $S = 3$, $L = 3$, and $J = 0$) while that of Eu^{2+} is $^8S_{7/2}$ ($4f^7$; $S = 7/2$, $L = 0$, and $J = 7/2$). The contribution from the ground state of Eu^{3+} to the susceptibility is explicitly zero and the van Vleck terms from higher multiplets contribute to the susceptibility. The mixing of excited states of $4f^6$ produces a weak temperature-dependent contribution to the magnetic susceptibility.[26] As the energy splitting Δ/k_B between $J = 0$ and $J = 1$ states for Eu^{3+} depends on the environment of the Eu ion, we analyzed the contribution from the $J = 1$ excited state with different values of Δ/k_B and calculated the susceptibility. The calculated susceptibility is almost consistent with other Eu^{3+}-based materials and the calculation in Ref. 26. Thus, we used a typical energy-splitting value of $\Delta/k_B \sim 540$ K.[26,27] Actually, the van Vleck paramagnetic susceptibility of the Eu^{3+} state around room temperature is almost independent of Δ/k_B. The measured magnetic susceptibility may be expressed as follows:

$$\chi^{\mathrm{obs}} = (1-\varepsilon)\,\chi^{\mathrm{C}}_{\mathrm{Eu}^{2+}} + \varepsilon\chi^{\mathrm{vV}}_{\mathrm{Eu}^{3+}} + \chi^{\mathrm{ESR}}_{\mathrm{Pauli}}, \qquad (1)$$

where the χ^{obs} is the observed susceptibility, $\chi^{\mathrm{C}}_{\mathrm{Eu}^{2+}}$ and $\chi^{\mathrm{vV}}_{\mathrm{Eu}^{3+}}$ are the calculated Curie susceptibility for Eu^{2+} and the van Vleck paramagnetic susceptibility for Eu^{3+}, respectively, $\chi^{\mathrm{ESR}}_{\mathrm{Pauli}}$ is the Pauli susceptibility estimated from the ESR integrated intensity, and ε is the contribution from the fraction of the Eu^{3+} state. The $\chi^{\mathrm{ESR}}_{\mathrm{Pauli}}$ for the conduction electrons is estimated to be $\sim 1.31 \times 10^{-2}$ (emu/mol). Using Eq. (1), the averaged valence of Eu atoms, $+2\,(1-\varepsilon) + 3\varepsilon = (2+\varepsilon)$, is found to be about 2.23 at 300 K. The contribution from higher multiplets of the Sm^{2+} state, which have the same electronic configuration as the Eu^{3+} state, is also described in Ref. 21. The calculated susceptibility for the Sm^{2+} state is almost the same order of magnitude as the Eu^{3+} state and the value of ε in $Eu_{2.75}C_{60}$ is similar to that of $Sm_{2.75}C_{60}$.

As shown in Fig. 2(a), the magnetic susceptibility is weakly dependent on temperature from 295 to 100 K. The temperature-independent susceptibility was almost consistent with the ESR results, as shown hereinafter. The solid green line in Fig. 2(a) is the calculated result for the Curie contribution from the free

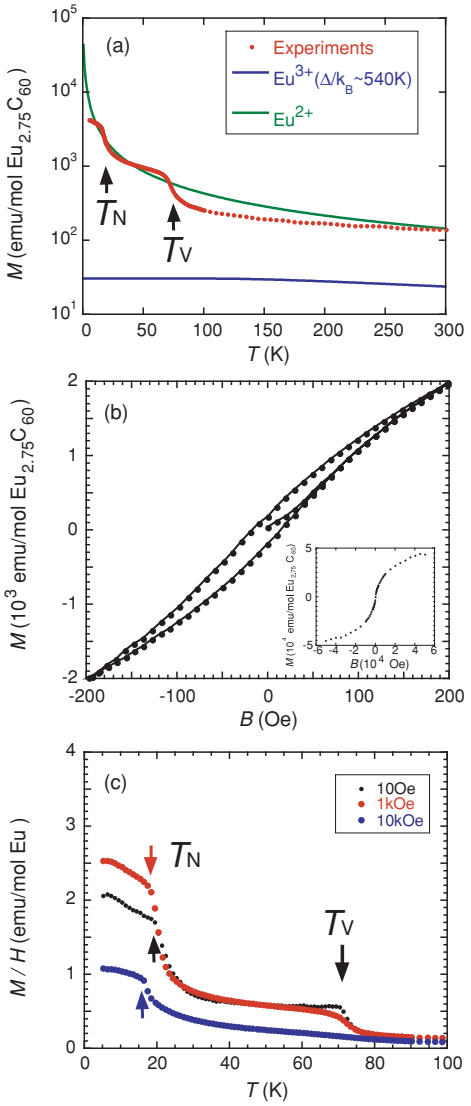

FIG. 2. (Color online) (a) Comparison of measured temperature-dependent magnetization with calculation. The solid green line is the calculated result for the divalent Eu state ($4f^7$; $S = 7/2$, $L = 0$, and $J = 7/2$) and the solid blue line is that for the trivalent Eu state with $\Delta/k_B = 540$ K ($4f^7$; $S = 7/2$, $L = 0$, and $J = 7/2$). From T_V to 20 K, the measured susceptibility can be fit by the Curie-Weiss law with a Weiss constant of ~56 K. The magnetization is measured at a magnetic field of 2000 Oe. (b) Low-field part of isothermal magnetization at 5 K, where a small hysteresis is shown. The inset shows the whole isothermal magnetization. (c) Temperature dependence of magnetization at different magnetic fields.

Eu^{2+} ion ($4f^7$; $S = 7/2$, $L = 0$, and $J = 7/2$) and the solid blue line is that for the van Vleck paramagnetism of the free Eu^{3+} ion. At high temperatures, the observed susceptibility follows a curve between those expected for the two valence states, which implies the intermediate valence state of Eu. In contrast, below 70 K, the magnetic susceptibility almost follows the Curie susceptibility from the free Eu^{2+} ion. Thus, at least, the Eu^{2+} state is probably more dominant than the Eu^{3+} state at $T < T_V$, where T_V is the valence transition temperature. This result is consistent with the thermally expanded lattice constant below T_V because of the larger ionic radius of the Eu^{2+} ion compared with the Eu^{3+} ion. The slight difference between measured susceptibility and the calculated Curie susceptibility from the free Eu^{2+} ion in the region below T_V is attributed to the Curie-Weiss behavior in the experiments. The Weiss constant is found to be ~56 K, which suggests the existence of antiferromagnetic correlations between C_{60} molecules, between Eu atoms, and/or between Eu and C_{60}. The susceptibility around T_V displays a weak thermal hysteresis (not shown). This result suggests that the phase transition at T_V may be first order, which is consistent with the thermal lattice-expansion experiments [Fig. 1(b)].

Several rare-earth compounds exhibit valence fluctuating phenomena. Extensive studies have shown that EuM_2X_2 (M = transition metal, X = Si, Ge, or P) undergoes a temperature- and pressure-induced valence transition.[28] In $EuCo_2P_2$, at ambient pressure, the ground state of Eu is divalent and Co has no magnetic moment.[29] Although the nonmagnetic ground state (i.e., the Eu^{3+} state) may be basically preferred at lower temperature, the valence state of Eu strongly depends on the location of 3d-band states relative to the Fermi energy E_F, producing interesting valence states. Because of the observation of the ESR signal, which can be attributed to the π conduction electrons, the t_{1u} band of C_{60} should be partially filled and the coupling between the t_{1u} band of C_{60} and Eu $4f$ states may play an important role in determining the Eu valence (i.e., the appearance of Eu^{2+}).

The magnetizations show a clear anomaly around $T_N = 17$ K. Below T_N, the isothermal magnetization shows a weak hysteresis loop as a function of the magnetic field. Figure 2(b) shows the magnetization curve at 5 K. These results suggest that $Eu_{2.75}C_{60}$ undergoes a magnetic phase transition at T_N. The isothermal magnetization below T_N indicates a weak ferromagnetic component produced in the magnetically ordered structure. Therefore, we propose an antiferromagnetic ground state with a weak ferromagnetic component below T_N for $Eu_{2.75}C_{60}$. Note that this magnetic transition temperature is higher than the ferromagnetic transition temperature of Eu_6C_{60} ($T_C = 11.6$ K).[30]

Figure 2(c) shows the temperature dependence of magnetization at different magnetic fields. The Néel temperature T_N deceases slightly with increasing magnetic field. This should be the typical behavior around T_N for an antiferromagnet. Moreover, we emphasize that the magnetic susceptibility below T_V is sensitive to the magnitude of the applied magnetic field. Nonlinear magnetizations under magnetic fields are observed below T_V. When the magnetic field is sufficiently increased, the low-temperature susceptibility below T_V decreases and the anomaly at T_V becomes indistinct. Because the susceptibility above T_V is almost unchanged, the valence state in the region above T_V is suggested to be unaffected by the magnetic field under these experimental conditions. On the contrary, the susceptibility below T_V indicates that the valence state is modified by the magnetic field (i.e., the fraction in the Eu^{2+} state that contributes to the Curie term) and deceases at higher magnetic field. Basically, the Eu^{2+} state may be more stable than the Eu^{3+} state at high field because of their different magnetic moments for ground-state multiplets. If this is the case, the fraction of the Eu^{3+} state should decrease with increasing field, which results in the increase of susceptibility. However, the magnetization below T_V is clearly suppressed at

high magnetic field. This result still remains to be clarified at the present stage. A detailed search for valence change under magnetic fields is necessary to clarify this problem.

We now discuss the origin of the antiferromagnetic interaction. We have pointed out three possible interactions between C_{60} molecules, between Eu atoms, and/or between Eu and C_{60}. When the magnetic interaction between Eu atoms is dominant, T_N may be markedly decreased because of the decrease in the magnetic moment of the Eu state at high field. In spite of the drastic suppression of the magnetic susceptibility below T_V at high magnetic field, T_N scarcely decreases at high magnetic field, as described above. Therefore, magnetic interactions between C_{60} might dominantly contribute to the low-temperature magnetic susceptibility (i.e., the magnetic ground-state configuration is determined by the interactions between C_{60}s).

A typical ESR spectrum of $Eu_{2.75}C_{60}$ at 290 K is shown in the inset of Fig. 3(a). The spectrum is composed of two lines with Lorentzian line shapes, one of which is a broad line with a peak-to-peak line width ΔB_{pp} of 1110 Oe and the other is a narrow line with ΔB_{pp} of 3.1 Oe. The g factors for these broad and narrow lines are 2.0288 and 2.0050, respectively. These signals possibly originate from either π spins in C_{60} or 4f spins in Eu^{2+} because the observed g factors are close to 2 and the ground state of Eu^{3+} is spin-silent ($^7F_0$). In ternary Eu pnictides EuCuP and EuAuSb,[31] where the Eu ions have temperature-independent valence states close to divalent, the ESR signals of the bulk Eu^{2+} state have been observed. The ESR line-widths for EuCuP and EuAuSb were found to be about 800 Oe and 3000 Oe, respectively and their spin susceptibilities estimated by ESR integrated intensities were consistent with those obtained from dc magnetic susceptibility. Although the broad line-width obtained in $Eu_{2.75}C_{60}$ is comparable with that obtained from EuCuP and EuAuSb, the small spin susceptibility estimated by the integrated ESR intensity in $Eu_{2.75}C_{60}$ is not coincident with that obtained from the dc magnetic susceptibility. The Lorentzian line shape of the observed ESR signals implies that the penetration depth of microwaves is larger than the grain size of the samples. Therefore, we can exclude the possibility of underestimation of spin susceptibility due to the experimental uncertainties. We conclude that the broad line should be assigned to intrinsic π spins on C_{60} in $Eu_{2.75}C_{60}$ because of the weak ESR intensity as well as on the basis of the assignments in the ESR of other metal-ion-doped C_{60} materials.[32] The observed g shift from 2 for the broad ESR signals should be due to spin-orbit coupling through π-4f (or 5d) mixing. However, the narrow line may be assigned to either defect π spins or 4f spins of Eu^{2+} because their intensity is weaker than the intrinsic broad line. It is interesting that the appearance of a broad ESR signal of π spin on C_{60} implies partial filling of the t_{1u} band of C_{60} at high temperatures.

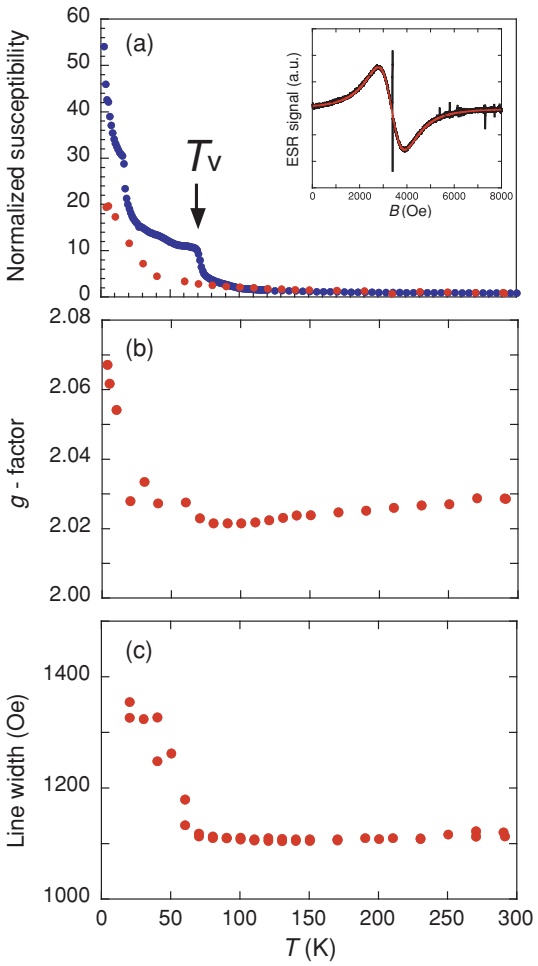

FIG. 3. (Color online) (a) Temperature dependencies of susceptibilities, which are normalized by the room temperature data. The susceptibilities estimated from ESR integrated intensity and SQUID measurements are indicated by red and blue circles, respectively. The inset shows a typical ESR signal at room temperature. The fitting curve for the broad line is shown by the red line. Temperature dependencies of ESR g-factor (b) and ESR peak-to-peak line width (c).

Figures 3(a)–3(c) show the temperature dependence of ESR parameters for $Eu_{2.75}C_{60}$. The integrated intensity of the broad ESR line increases slightly from 290 to 70 K, suggesting the itinerant nature of π electrons in C_{60} (i.e. Pauli-like behavior). The weak Korringa-like temperature variation of line-width supports this scenario. However, below T_V, the ESR integrated intensity increases rapidly. This Curie-type increase of integrated intensity possibly supports the localization of π electrons below T_V. This temperature corresponds well to the onset temperature of negative thermal expansion in $Eu_{2.75}C_{60}$. Plots of g as a function of temperature also show a drastic change around T_V (i.e., g gradually decreases with decreasing temperature down to T_V, and then rapidly increases below T_V). The rapid increase of the g factor suggests an enhancement of the contribution from the spin-orbit interaction due to the increase of the π-4f (or 5d) interaction. The quantity ΔB_{pp} shows an almost constant value above T_V, while it gradually increases below T_V from 1055 to 1600 Oe. Both the magnetic susceptibility and the ESR parameters clearly show an electronic transition at T_V in $Eu_{2.75}C_{60}$, which should be associated with the structural change in $Eu_{2.75}C_{60}$ caused by the Eu valence change. This structural change induces the localization of π electrons and the increase of the π-4f interaction. The insertion of Eu^{2+}, with its large ionic radius, increases the intermolecular distance between C_{60}s and possibly reduces the t_{1u} bandwidth. We expect

that the reduction of the t_{1u} bandwidth may lead to the enhancement of electronic correlations, which should be responsible for the localization of π electrons around T_V (i.e., a Mott-Hubbard transition). At T below T_V, the spin freedom on C_{60} should remain and can order antiferromagnetically below T_N.

IV. CONCLUSION

Our magnetic study of $Eu_{2.75}C_{60}$ implies that the valence ordering of the Eu atom occurs simultaneously with the structural phase transition at ~70 K. We also found that, at low temperature, valence-ordered $Eu_{2.75}C_{60}$ underwent magnetic ordering with a weak ferromagnetic component below ~17 K. The drastic change in ESR parameters below 100 K should reflect a variation of the conduction-electronic state caused by the valence transition of Eu atoms from the mixed-valence state of Eu^{2+} and Eu^{3+} to the single state of Eu^{2+} (i.e., valence fluctuation). Our results suggest that the valence fluctuation in $Eu_{2.75}C_{60}$ changes both the carrier concentration of the conduction band and the balance of electronic correlations, U/W, where U and W are Coulomb repulsion and band width, because of the different ionic sizes between Eu^{2+} and Eu^{3+}. The carrier concentration as well as the U/W balance are now inclined toward the appearance of an antiferromagnetic ground state. Thus, the $Eu_{2.75}C_{60}$ phase may be close to the Mott-transition and may have the potential to produce a novel quantum phase (e.g., a coexisting phase of magnetic ordering and superconductivity found in heavy-fermion systems) by a precise control of carrier concentration.

ACKNOWLEDGMENTS

The x-ray diffraction patterns were measured in research projects (2004G050, 2006G256, and 2007G612) of KEK-PF. This study was partly supported by a Grant-in-Aid (18340104) from MEXT, Japan.

*Present address: Graduate School of Engineering Science, Osaka University, 1-3 Machikaneyama-cho, Toyonaka 560-8531, Japan.
†Present address: Japan Synchrotron Radiation Research Institute, SPring-8, Hyogo 679-5198, Japan.
‡Corresponding author: kambe@science.okayama-u.ac.jp

[1] A. F. Hebard, M. J. Rosseinsky, R. C. Haddon, D. W. Murphy, S. H. Glarum, T. T. M. Palstra, A. P. Ramirez, and A. R. Kortan, Nature (London) **350**, 600 (1991).
[2] K. Tanigaki, T. W. Ebbesen, S. Saito, J. Mizuki, J. S. Tsai, Y. Kubo, and S. Kuroshima, Nature (London) **352**, 222 (1991).
[3] M. S. Dresselhaus, G. Dresselhaus, and P. C. Eklund, *Science of Fullerenes and Carbon Nanotubes* (Academic Press, 1995).
[4] T. Yildirim, O. Zhou, and J. E. Fischer, in *The Physics of Fullerene-Based and Fullerene-Related Materials*, edited by W. Andreoni (Kluwer Academic Publishers, 2000) p. 67.
[5] Y. Iwasa and T. Takenobu, J. Phys. Condens. Matter. **15**, R495 (2003).
[6] T. T. M. Palstra, O. Zhou, Y. Iwasa, P. E. Sulewski, R. M. Fleming, and B. R. Zegarski, Solid State Commun. **93**, 327 (1995).
[7] Y. Yoshida, Y. Kubozono, S. Kashino, and Y. Murakami, Chem. Phys. Lett. **291**, 31 (1998).
[8] S. Fujiki, Y. Kubozono, S. Emura, Y. Takabayashi, S. Kashino, A. Fujiwara, K. Ishii, H. Suematsu, Y. Murakami, Y. Iwasa, T. Mitani, and H. Ogata, Phys. Rev. B **62**, 5366 (2000).
[9] S. Fujiki, Y. Kubozono, M. Kobayashi, T. Kambe, Y. Rikiishi, S. Kashino, K. Ishii, H. Suematsu, and A. Fujiwara, Phys. Rev. B **65**, 235425 (2002).
[10] A. Y. Ganin, Y. Takabayashi, Y. Z. Khimyak, S. Margadonna, A. Tamai, M. J. Rosseinski, and K. Prassides, Nat. Mater. **7**, 367 (2008).
[11] Y. Takabayashi, A. Y. Ganin, P. Jeglič, D. Arčon, T. Takano, Y. Iwasa, Y. Ohishi, M. Takata, N. Takeshita, K. Prassides, and M. J. Rosseinsky, Science **323**, 1585 (2009).
[12] K. Prassides, in *The Physics of Fullerene-Based and Fullerene-Related Materials*, edited by W. Andreoni (Kluwer Academic Publishers, 2000) p. 175.
[13] O. Chauvet, G. Oszlànyi, L. Forró, P. W. Stephens, M. Tegze, G. Faigel, and A. Jànossy, Phys. Rev. Lett. **72**, 2721 (1994).
[14] A. Jànossy, N. Nemes, T. Fehér, G. Oszlànyi, G. Baumgartner, and L. Forró, Phys. Rev. Lett. **79**, 2718 (1997).
[15] Y. Kubozono, H. Maeda, Y. Takabayashi, K. Hiraoka, T. Nakai, S. Kashino, S. Emura, S. Ukita, and T. Sogabe, J. Am. Chem. Soc. **118**, 6998 (1996).
[16] T. Inoue, Y. Kubozono, S. Kashino, Y. Takabayashi, K. Fujitaka, M. Hida, M. Inoue, T. Kanbara, S. Emura, and T. Uruga, Chem. Phys. Lett. **316**, 381 (2000).
[17] T. Kanbara, Y. Kubozono, Y. Takabayashi, S. Fujiki, S. Iida, Y. Haruyama, S. Kashino, S. Emura, and T. Akasaka, Phys. Rev. B **64**, 113403 (2001).
[18] R. Klingeler, C. Breuer, I. Wirth, A. Blanchard, P. S. Bechhold, M. Neeb, and W. Eberhardt, Surf. Sci. **553**, 95 (2004).
[19] R. Klingeler, G. Kann, I. Wirth, S. Eisebitt, P. S. Bechthold, M. Neeb, and W. Eberhardt, J. Chem. Phys. **115**, 7215 (2001).
[20] X. H. Chen and G. Roth, Phys. Rev. B **52**, 15534 (1995).
[21] J. Arvanitidis, K. Papagelis, S. Margadonna, K. Prassides, A. N. Fitch, Nature (London) **425**. 599 (2003).
[22] J. Arvanitidis, K. Papagelis, S. Margadonna, and K. Prassides, Dalton Trans. **19**, 3144 (2004).
[23] K. Prassides, Y. Takabayashi, and T. Nakagawa, Philos. Trans. R. Soc. London A **366**, 151 (2008).
[24] S. Margadonna, J. Arvanitidis, K. Papagelis, K. Prassides, Chem. Mater. **17**, 4474 (2005).
[25] A. C. Larson and R. B. Von Dreele, *General Structure Analysis System (GSAS)*, Los Alamos National Laboratory Report LAUR 86 (2000).
[26] Y. Takikawa, S. Ebisu, and S. Nagata, J. Phys. Chem. Solids **71**, 1592 (2010).
[27] S. Rosenkranz, M. Medarde, F. Fauth, J. Mesot, M. Zolliker, A. Furrer, U. Staub, P. Lacorre, R. Osborn, R. S. Eccleston, and V. Trounov, Phys. Rev. B **60**, 14857 (1999).
[28] M. Reehuis and W. Jeitschko, J. Phys. Chem. Solids **51**, 961 (1990).

[29]M. Chefki, M. M. Abd-Elmeguid, H. Micklitz, C. Huhnt, W. Schlabitz, M. Reehuis, and W. Jeitschko, Phys. Rev. Lett. **80**, 802 (1998).

[30]K. Ishii, A. Fujiwara, H. Suematsu, and Y. Kubozono, Phys. Rev. B **65**, 134431 (2002).

[31]V. Kataev, G. Khaliullin, G. Michels, C. Huhnt, E. Holland-Moritz, W. Schlabitz, and A. Mewis, J. Magn. Magn. Mater. **137**, 157 (1994).

[32]L. Forró and L. Mihaly, Rep. Prog. Phys. **64**, 649 (2001).